Effect of Substitutional N on Important Chemical Vapor Deposition Diamond Growth Steps

T. Van Regemorter and K. Larsson*

Department of Materials Chemistry, Angstrom Laboratory, Uppsala University, Box 538, SE-751 21 Uppsala, Sweden

Received: December 31, 2008; Revised Manuscript Received: February 7, 2009

This study analyses theoretically the effects of substitutional N on three different chemical vapor deposition diamond growth steps. The investigation is based on density functional theory, using both cluster and periodic models. The reaction steps, assumed to be predominantly occurring during diamond growth, are (i) CH_2 insertion within a carbon dimer, (ii) H transfer from a neighboring surface carbon to an adsorbed CH_2, and (iii) surface migration of CH_2. Carbon atoms at various lateral positions are substituted by N within the second, third, and fourth carbon layers beneath the surface. Both reaction energies and barrier energies were for all reaction steps carefully calculated. For the CH_2 insertion into a carbon dimer, the reaction energy was found to be in principle unaffected by substitutional N. However, the activation energy for the CH_2 insertion reaction was with one exception observed to be significantly increased by the presence of substitutional N. The H migration reaction was only found to be sensitive to the lateral position of N in the carbon layers. The reaction is observed to be favored or disfavored depending on this lateral position. For the CH_2 migration reaction, the substitutional N was observed to increase the activation barriers and thereby negatively affect the reaction kinetics.

I. Introduction

The entire control of diamond texture and morphology at a sufficiently high CVD (chemical vapor deposition) growth rate is a challenging goal aimed for by researchers for many years.[1−3] The achievement of a diamond film with desired properties and morphology will, however, require a perfect recognition of the parameters affecting the growth process (e.g., substrate temperature, methane concentration, presence of impurities, etc.).[4−6] It is especially crucial to understand how these parameters will affect the growth on an atomic level.

Locher et al.[7] and Jin and Moustakas[8] were the first ones to observe (1994) that the presence of nitrogen in the gas phase strongly affects the growth. It is especially observed that the growth rate will be enhanced, and the surface morphology will exhibit a more pronounced (100) texture, for a small N/C ratio.[9] For larger N concentrations, a deterioration of the surface, which becomes nanocrystalline, is then generally observed. This effect is generally explained by an increase in secondary nucleation and a higher concentration of sp^2 carbon in the diamond film.[10,11] Besides the large amount of experimental works, only few theoretical studies have been devoted to this topic, and the important effect of nitrogen on growth is still not fully understood. Recently, Butler et al. have proposed that the diamond (111) growth rate will increase when the CN species is present in the gas phase.[12] Within previous theoretical studies on the diamond growth mechanism, these authors have furthermore suggested that the nucleation of a new carbon layer is the rate limiting step.[13,14] They proposed that adsorbed CN will enhance this new layer nucleation. While this observation is interesting for the (111) surface orientation, it is not straightforward to transfer their explanation to another surface orientation like (100). Frauenheim et al. proposed that the increased diamond (100) growth rate is induced by the presence of a substitutional N into the diamond lattice. From bulk studies, it is well-known that substitutional N will induce a lattice distortion due to the occupation of an antibonding C−N orbital by the "extra" electron in N (compared to C).[15−17] When an empty, or partially empty, state is available in the band gap (e.g., originating from radical surface sites), it is observed that the extra nitrogen electron will be easily transferred toward this available state and thereby stabilize the diamond structure (i.e., the lattice distortion disappears).[18,19]

In a recent theoretical study by the present authors, the effects of substitutional N on CH_3 adsorption, and on H abstraction from CH_3, have been theoretically studied.[20] Important variations in reaction efficiency were especially observed when positioning N in the second atomic C layer. In general, substitutional N was observed to energetically disfavor the CH_3 adsorption reaction and favor the H abstraction from the adsorbed CH_3 species. Further analysis relates this effect with the possibility for the nitrogen's extra electron to be transferred toward a surface radical carbon. For some specific cases where N was positioned in the β-position with respect to the surface radical carbon (i.e., there is one carbon between N and the radical carbon), a β-scission reconstruction was observed to take place (i.e., the N−C bond is broken in favor of the formation of a C−C double bond). This formation of a sp^2 carbon was proposed to be correlated to the surface degradation that has experimentally been observed for a large N concentration.

The purpose of this study is to get a deeper understanding of how the presence of substitutional N will affect three important elementary reaction steps within the CVD diamond growth process. The first reaction is the insertion of an already adsorbed CH_2 species into a surface carbon dimer (reaction step 1). This reaction step is generally considered as very crucial for the diamond growth mechanism.[21−23] An H transfer reaction between the adsorbed CH_2 species and a neighboring surface carbon (reaction step 2) is also considered as an important step for diamond growth.[24,25] The reaction step 3 constitutes the surface migration of a CH_2 species, which is a process that may be of large importance for a step flow type of diamond growth.[26] For all these three elementary reaction steps, elemental C at

10.1021/jp811505w CCC: $40.75
Published on Web 03/04/2009

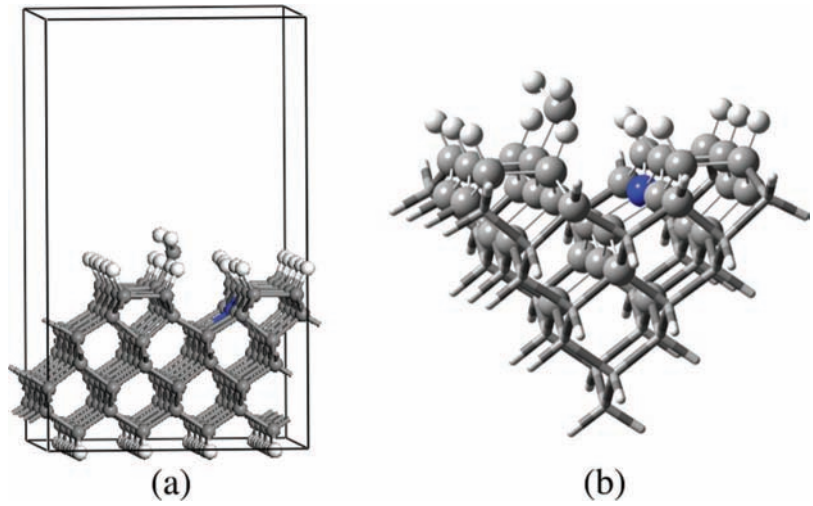

Figure 1. Representations of the models used to simulate the (100)-2 × 1 diamond surface: (a) a periodic model that was used in the DMol[3] calculations and (b) a cluster model used for the Gaussian 03 calculations. In both cases, the surface is fully H-terminated with an adsorbed CH_2 species. For the cluster model, the atoms represented with ball and sticks are allowed to relax during the geometry optimization, while the atoms represented with sticks are frozen to simulate the diamond bulk.

various positions within different carbon layers beneath the surface is substituted by N. In this way, not only is the effect by the elemental N looked for, but also the eventual tendency for a somewhat longer range effect.

II. Model and Computational Method

1. General. The calculations were based on the density functional theory (DFT) method, using two different software programs: the program package DMol[3] from Accelrys, Inc.[27] and the Gaussian 03 suite of programs.[28] The DMol[3] program works under periodic boundary conditions and uses localized numerical basis sets, while Gaussian 03 uses cluster models and localized basis sets. In the present study, both of these DFT softwares have been used for calculating reaction energies and thereby the thermodynamic driving force for the reactions to take place. However, a complete energetic reaction profile should also contain kinetic information by including an estimation of the energetic barriers for the reactions. These energies could here only be calculated by using Gaussian 03. The reaction energies (ΔE) were calculated using the following equation

$$\Delta E = E_{\text{prod}} - E_{\text{react}} \quad (1)$$

where E_{prod} and E_{react} are the energies calculated for the product and the reactant surface structure, respectively. Similarly, the activation energies were calculated with the following equation

$$\Delta E^* = E_{\text{TS}} - E_{\text{react}} \quad (2)$$

where E_{TS} is the energy calculated for the transition state structure.

2. Surface Models. When using DMol[3], a periodic boundary model represents the (100)-2 × 1 H-terminated diamond surface using a unit cell with a length of 10.06 Å in the *x*- and *y*-directions, and 16.65 Å in the *z*-direction (cf. Figure 1a). Due to the infinite repetition of this unit cell in three directions, the diamond surface is represented by an infinite slab in the *x*- and *y*-directions with a thickness of 6.65 Å, corresponding to 7 atomic carbon layers (i.e., a total of 108 carbon atoms per unit cell). The two lowest carbon layers were frozen to simulate the diamond bulk, and all dangling bonds were terminated with H. The vacuum layer was set to 10 Å, which has earlier been found to be adequate in avoiding interactions between two repeating slabs in the *z*-direction.[29]

The cluster model used for the Gaussian 03 calculations (Figure 1b) contains 62 carbon atoms. This cluster has been cut out from a periodic model optimized using DMol[3], and all unsaturated carbon bonds were terminated with H. In order to simulate the bulk diamond beneath the surface, some of the atoms were frozen during the geometry optimization. As can see in Figure 1b, the atoms and bonds that are represented with balls and sticks were free to relax, while the others were constrained.

3. Theoretical Methods. For the DMol[3] program, the calculations were based on the spin-polarized general gradient approximation using the BLYP functional (a hybrid functional where the exchange and correlation parts are generated by B88[30] and LYP,[31] respectively). The geometry optimizations were performed using the BFGS algorithm.[32] A mesh of (2 × 2 × 1) k-points was generated using the Monkhorst−Pack scheme,[33] and the SCF density convergence was set to 1.00×10^{-6}. The numerical basis set of choice included polarization p-functions on all hydrogen atoms and d-functions on all carbon and nitrogen atoms.

The Gaussian 03 calculations were performed using the B3LYP hybrid functional, where the electron exchange part is described using the Becke three parameter hybrid functional[34] and the electron correlation part is described by the LYP functional. The C atoms that are either directly involved in the surface reactions or surrounding the substitutional N atom were allowed to relax during the geometry optimization procedure and were also represented by a Pople type of basis set with additional polarization functions, 6-31G(d,p). This latter optimization procedure was based on redundant internal coordinates, and the search for transition states was performed using the synchronous transit-guided quasi-Newton (STQN) method.[35]

In order to understand the underlying causes for the observed energetic differences, the analysis of structural changes has been complemented with an atomic population analysis with the purpose of investigating the electronic structure of the system.

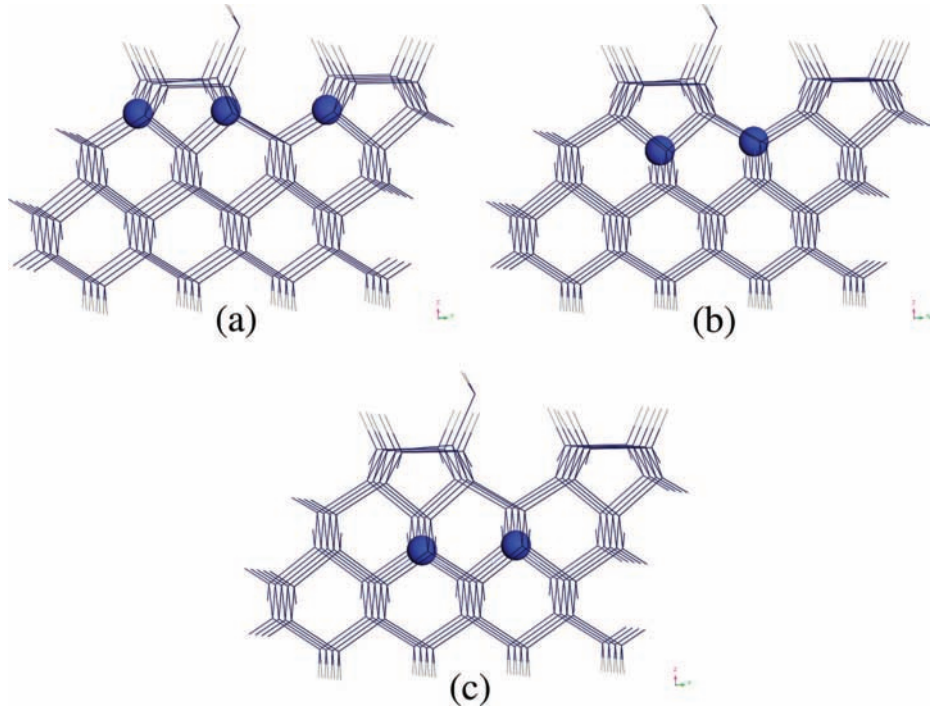

Figure 2. Representations of the N position in the second (a), third (b), and fourth (c) carbon layers. For the second carbon layer, the positions are labeled 1, 2, and 3 from right to left, and for the thirrd and the fourth carbon layers the N positions are labeled 1 and 2 from right to left.

This analysis was performed using the natural atomic orbitals (NAO) analysis (using the NBO (v3.1) program within Gaussian 03).[36]

The effects of substitutional N on the (i) CH_2 insertion into a C−C dimer, (ii) H surface migration, and (iii) CH_2 surface migration were considered for N in three different positions within the second carbon layer. It was also considered for N in two different positions within the third and fourth carbon layer, respectively. All these N positions are represented in Figure 2. From here on, the surface with specific positions of N will be presented as NL*x*P*y*, where *x* and *y* represent the positions of N in the y^{th} position within the x^{th} atomic layer.

III. Results

1. General. The diamond CVD growth process occurs through a complex set of elementary reaction steps on the surface.[5] The reaction between gaseous hydrogen radicals (H) and the diamond surface is one of the most important steps. The H species is crucial for the abstraction of an adsorbed H (with the formation of H_2 molecules) in order to form a surface carbon radical. The formation of these surface radicals are absolutely necessary for the adsorption of gaseous growth species to take place, here considered as the CH_3 radical. Moreover, further removal of H from the adsorbed methyl species has to take place. As one alternative, this can take place by abstraction reaction using a gaseous H radical. Another alternative for the formation of the CH_2 adsorbate is the migration of H (in CH_3) toward a neighboring surface C radical. The resulting CH_2 adsorbate is thereafter assumed to be inserted within a surface carbon dimer. This so-called inserted CH_2 might thereafter migrate on the surface toward a surface step, where the carbon will finally be incorporated into the lattice.

The insertion reaction within a carbon dimer is generally described as occurring in two steps: (a) a dimer opening step which forms an intermediate "open-ring" structure and (b) a ring closing step.[21,22,37] The open-ring structure has earlier been calculated to be stable using either DFT methods with a small cluster[38] or classical[21] and semiempirical[22] methods using a large model. However, a careful study using complete active space self-consistent field wave functions (CASSCF), and the multireference second order perturbation theory (MRPM2), showed that this intermediate open-ring structure is expected to have a short lifetime.[23]

The possibility for surface migration by atomic H has earlier been discussed in several theoretical studies.[24,25,37,39] More specifically, it has been observed that H is easily migrating between a neighboring surface carbon radical and (i) a monatomic step, (ii) a dihydride unit on (100) surfaces, or (iii) a chemisorbed hydrocarbon species.[24,40,41] The H migration from an adsorbed CH_3 to a neighboring radical carbon is, for the formation of an adsorbed CH_2, often considered as an alternative mechanism to H abstraction from CH_3.[24,25,42] This reaction step is thereby important for the entire growth process, and the eventual changes induced by the presence of a substitutional N need to be considered.

Evidence for a step flow growth has experimentally been confirmed for certain appropriate conditions.[43−45] These observations are generally explained by two specific mechanisms. The first one introduces the concept of "preferential etching" of an isolated CH_2 species with the support from atomic H. The CH_2 adsorbed next to a step is considered to be more easily incorporated into the lattice.[46] The other proposed mechanism introduces the migration of the CH_2 species toward a step, where it gets finally incorporated.[37,39,47] As proposed recently by D'Evelyn et al., since the two models present their own limitations, both etching and short-range migration might occur during growth of diamond.[48] Based on these observations, the migration of a CH_2 species from an inserted position within the C−C dimer toward a bridged position between two carbon dimers is of major importance and should be more carefully investigated.

The effect of substitutional N on CH_3 adsorption, and on H abstraction from the CH_3 adsorbate, has very recently been studied by the present authors.[20] As a natural continuation within

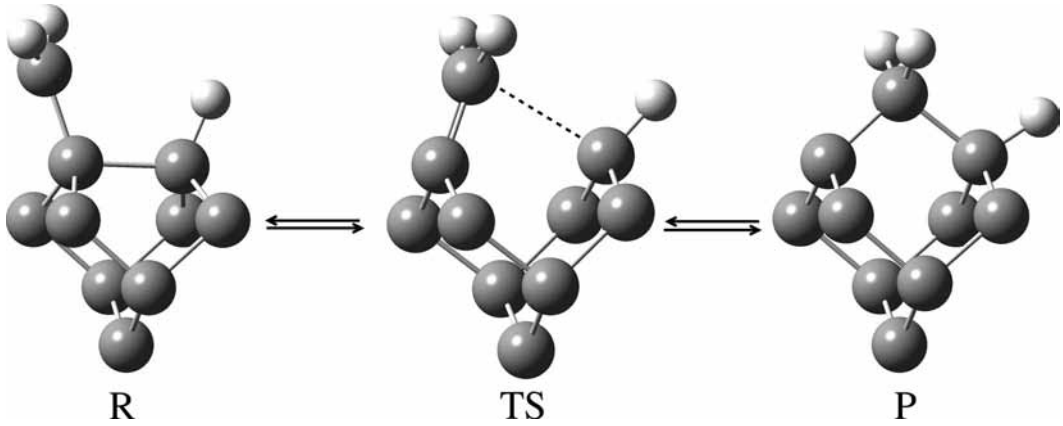

Figure 3. Mechanism describing the incorporation of an adsorbed CH_2 into a carbon dimer. R, P, and TS denote the reactant, product, and transition state structure of the reaction, respectively.

TABLE 1: Reaction Energies (ΔE) and Activation Barriers (ΔE^*) for CH_2 Incorporation into the Carbon Dimer[a]

energies (kJ/mol)	no nitrogen	NL2P1	NL2P2	NL2P3	NL3P1	NL3P2	NL4P1	NL4P2
ΔE (DMol^3)	−20	−14	85	−11	−56	−105	−28	−32
ΔE (Gaussian03)	−37	−23	56	−39	−72	−139	−48	−
ΔE * (Gaussian03)	107	251	355	80	208	178	214	−

[a] The calculations have been performed with the programs DMol^3 and Gaussian 03, both with and without N in the lattice at various positions.

this series of investigations, the study presented here focuses on the effect of substitutional N on (i) CH_2 insertion into the C−C dimer, (ii) H migration between an adsorbed CH_2 and a neighboring surface radical, and (iii) migration of inserted CH_2 species. The main goal of this study is to investigate theoretically, using DFT methods, the effect of a substitutional N on these three important reactions which are assumed to occur during diamond CVD growth. Both thermodynamic and kinetic aspects of the reactions will be considered.

2. CH_2 Insertion into a Dimer. ***General.*** The insertion reaction of an adsorbed CH_2 into the surface carbon dimer is sketched in Figure 3. The ring closing step of the reaction is assumed to be the rate determining step due to its higher activation barrier, as discussed above, and is therefore the only reaction which is here presented and discussed.

Effect by Substitutional N on Reaction Energy. The calculated CH_2 insertion reaction energies, using both DMol^3 and Gaussian 03, are presented in Table 1. Even though the two methods used in the calculations are based on different approximations, and also used for different model types, it is obvious that they both result in an identical trend for the insertion reaction energy. This circumstance will thereby strongly support the present observations regarding the influence of N on the CH_2 insertion into a dimer.

As can be seen in Table 1, the presence of a substitutional N is generally not strongly affecting the energy of carbon dimer insertion reaction. However, two exceptions can be observed for the situations with N in position 2 in the second and the third carbon layers, respectively (the reaction energy is disfavored by 85 kJ/mol for NL2P2, and favored by 105 kJ/mol for NL3P2). In order to explain these energetic changes, the energy of the surface structures describing the situation of NL2P2 and NL3P2 prior to the dimer insertion is compared with the surface energies calculated for N in the second carbon layer in position 1 (NL2P1). An identical procedure is used for the final structures obtained after the CH_2 insertion reactions. From these analyses, the observed endothermicity of the reaction for N in the second carbon layer, position 2, is explained by a stabilization (about 157 kJ/mol) of the reactant structure. Similarly, the important exothermicity of the reaction with N in the third carbon layer, in position 2, is explained by a stabilization of the surface structure (about 111 kJ/mol) after the insertion reaction. Both of these exceptions can be explained by the presence of N in β-position with respect to a surface radical carbon, whereby a structural rearrangement of the surface occurs through a β-scission mechanism. For NL2P2 and before the insertion, the radical is positioned on the adsorbed CH_2, and for NL3P2 the radical is positioned on a surface carbon. The breakage of the C−N bond (B1 and B3) in favor of the formation of a double C−C bond (B2 and B4), sketched in Figures 4a and b, will strongly stabilize the surface structure.

With N in layer 3, position 2, it was possible to localize an additional intermediate structure which was otherwise not observed for the other situations. This structure is formed by two consecutive β-scission rearrangements on the surface prior to the insertion reaction. The breakage of the C−N bond (B5) induces the formation of an unsaturated C−C bond (B6) which, in turn, induces the cleavage of the surface carbon dimer (B7) and the formation of a second C−C double bond (B8; cf. Figure 4c). This structure is calculated to be more stable by about 27 kJ/mol compared to the reactant structure with CH_2 adsorbed on the surface.

For the other situations with N not being in β-position with respect to the surface radical (i.e., NL2P1, NL2P3, NL3P1, NL4P1, and NL4P2 in Table 1), the system cannot relax through a β-scission mechanism. It is instead observed to relax through the transfer of an electron from N to the surface radical carbon, and thereby induce the formation of an electron lone pair. This effect has very recently been observed in a previous work by the present authors, where the effect of N within the second carbon layer was investigated,[20] and is here confirmed to also occur for N positioned in the third and fourth carbon layers, respectively. For those situations where an electron transfer is taking place, the energies of the surface structures before and after the insertion reaction, and with N in different positions, have been compared with corresponding energies obtained for NL2P1. For NL2P2, only minor energetic differences have been observed with CH_2 inserted into the carbon dimer. In that

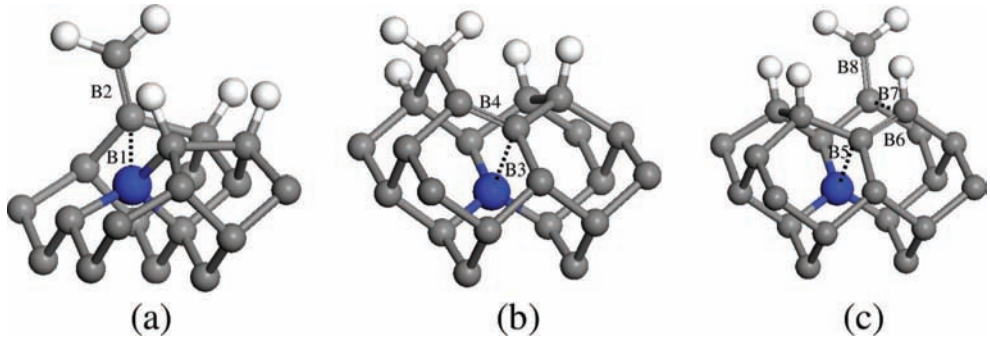

Figure 4. Representation of the β-scission reconstructions observed when a surface carbon radical is in β-position of N: (a) N in position 2 in the second carbon layer with CH_2 adsorbed on the surface, (b) N in position 2 in the third carbon layer with CH_2 inserted in the carbon dimer, and (c) N in position 2 in the third carbon layer.

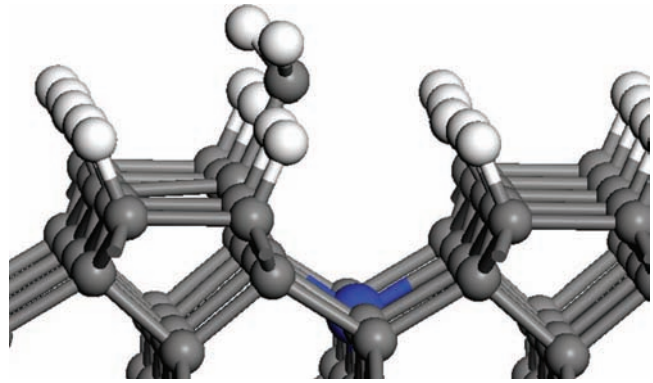

Figure 5. sp^3 configuration of the adsorbed CH_2 in the presence of substitutional N within the second, third, or fourth carbon layer.

specific case, N is directly connected to the surface radical and the surface is calculated to be more stable by about 55 kJ/mol.

The effect of this electron transfer process can be visualized by the geometry of the adsorbed CH_2 species (i.e., prior to the dimer insertion) in Figure 5. The geometry of an adsorbed CH_2 is planar for a nondoped diamond lattice, while the CH_2 geometry for the N-doped scenario shows evidence of sp^3 hybridization being induced by an electron transfer and the formation of a lone pair. This transfer is further confirmed by an NBO analysis, performed on the cluster model using Gaussian 03. The atomic charge on the C within the CH_2 adsorbate has evolved from -0.33 e for the undoped structure to about -0.95 e in the presence of N.

After the CH_2 insertion, the presence of N does not induce strong structural changes but the electron transfer is still visible. The NBO analysis shows that, without any dopant, the threefold coordinated surface carbon has an atomic charge of 0.09 e, while, in presence of substitutional N, the charge becomes much more negative (around -0.45 e). An exception is observed with N in the second carbon layer, position 2, and with CH_2 inserted within the carbon dimer. N is then directly bonded to the threefold coordinated surface C, which then presents a less negative atomic charge, -0.25 e.

In summary, the influence of a substitutional N (in β-position to a surface radical carbon) on the thermodynamics of the CH_2 insertion reaction has been clearly identified in the present study. When the surface reconstruction occurs, the diamond surfaces including sp^2 carbon atoms are observed to be energetically the most stable ones. In addition, the surfaces have been found to be more stable with N directly connected to the surface carbon radical. The CH_2 insertion reaction is thereby disfavored. For the other N positions, the insertion reaction energy was not found to be strongly affected.

Effect by Substitutional N on Activation Energy. The activation barrier for the CH_2 insertion reaction into the C−C dimer has been estimated using Gaussian 03, and the resulting energies are presented in Table 1. With one exception, the CH_2 insertion reaction is associated with a much larger activation barrier in the presence of substitutional N compared to the undoped situation (an increase within the range 77−248 kJ/mol). For the situation with N in the second carbon layer, position 3, the activation barrier is lowered by 27 kJ/mol.

The large barrier calculated for N in the second carbon layer position 2 (NL2P2), of about 355 kJ/mol, is explained by the β-scission rearrangement which strongly stabilizes the surface prior to insertion. For N in the third carbon layer, position 2 (NL3P2), the β-scission rearrangement that takes place during the insertion reaction is not affecting the kinetics of the forward reaction. Despite the large decrease observed for the reaction energy, the activation barrier is similar to the values obtained for the other N positions (i.e., the activation energy is 178 kJ/mol for NL3P2 vs 208 and 214 kJ/mol for NL3P1 and NL4P1, respectively). However, the presence of the intermediate structure for NL3P2 (as discussed above, in the second part of Section III.2) indicates the possibility for a second insertion mechanism which might energetically be more favorable. It is important to emphasize the strong influence on surface reactivity that surface structure stabilization might induce. For N in position 2 in the second carbon layer, the large activation energy that is needed to be overcome clearly shows how much the stabilization of the initial structure will affect the reaction kinetics.

For all other N positions considered, where no β-scission rearrangements where observed (i.e., NL2P1, NL2P3, NL3P1, NL4P1), the variations in activation barriers are related to the stability of the transition structures only. These energetic

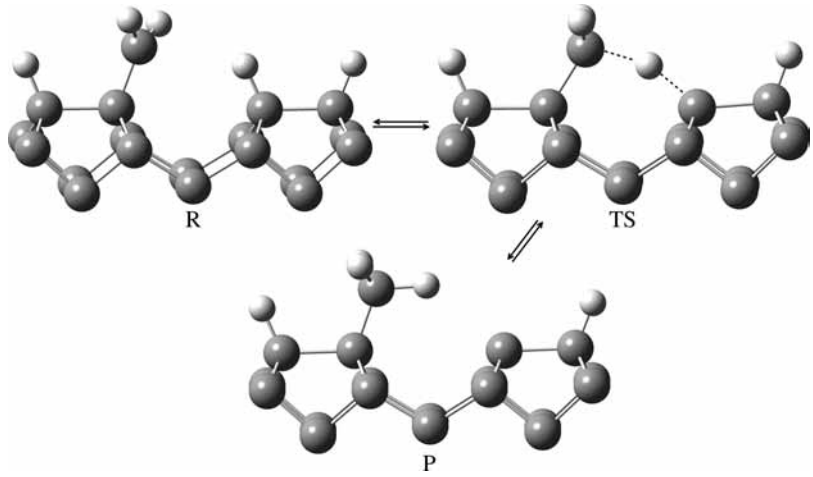

Figure 6. Representation of the H transfer reaction with R, TS, and P denoting reactant, transition state, and product structures, respectively.

TABLE 2: Reaction Energies for the H Transfer Reaction

H transfer (kJ/mol)	no nitrogen	NL2P1	NL2P2	NL2P3	NL3P1	NL3P2	NL4P1	NL4P2
ΔE (DMol^3)	9.9	−69.4	161.5	20.0	−17.0	16.8	−14.0	4.7
ΔE (Gaussian)	3.2	−86.7	169.5	55.3	−17.9	43.1	−16.3	−
ΔE* (Gaussian)	90.2	4.7	186.5	77.9	33.7	68.6	34.0	−

variations can be further investigated by careful analysis of geometrical structures and atomic charges (using the NBO program implemented in Gaussian 03) of the different carbon atoms involved in the reaction. As observed in Figure 3, the insertion reaction for a nondoped surface passes a transition state structure where the C−C dimer bond is broken and the C−CH_2 bond becomes shorter (around 1.35 Å, which is similar to the length of a C−C double bond: 1.34 Å[49]). In the presence of N, the extra electron transferred toward the surface will be localized on the surface C with which the CH_2 will form a new bond (represented by the dashed line within the TS structure in Figure 3). The atomic charge localized on this surface carbon (of about −0.74 *e* for N in the second, third, and fourth carbon layers, position 1) is much more negative compared to the undoped situation (−0.22 *e*). In addition, the charge of C within the adsorbed CH_2 is negative and is not much affected by the presence of N (about −0.36 *e* with N vs −0.40 *e* for the undoped lattice). In the presence of N, the more negative surface carbon will induce a stronger electrostatic repulsion between the two carbon atoms involved in the new bond formation (the bond is represented by the dashed line within the TS structure in Figure 3). The presence of this repulsion is confirmed by the longer distance between these two C (2.33 Å without N vs 2.80, 2.87, and 2.83 Å for N in the second, third, and fourth layers position 1, respectively). The more intense electrostatic repulsion observed in the presence of N will induce a destabilization of the TS structure, which explains the higher activation barriers. For N within the second carbon layer in position 3, where N is directly bonded to the surface C, the electronic charge appears to be less localized on the surface C within the transition structure (the charge is about −0.40 *e*), thereby reducing the electrostatic repulsion. This tendency is confirmed by a shorter distance between CH_2 and the surface carbon (2.36 Å) and furthermore explains the lower activation barrier observed for N in that position.

In conclusion, it appears that the major surface stabilization, induced by the formation of an sp^2 carbon species, will cause a significant increase in the activation barrier of the CH_2 insertion mechanism. When formed, the reconstructed surface may initiate the formation of defects. When N is not in β-position, the activation barrier for the CH_2 insertion into a C−C dimer is generally increased, thereby reducing the probability for the insertion reaction to take place. Substitutional N is thereby expected to hinder the growth.

3. H Transfer Reaction between an Adsorbed CH_2 and a Neighboring Surface Carbon. ***General.*** The H transfer reaction is sketched in Figure 6, and the calculated reaction energies and activation barriers are presented in Table 2.

The reactant structure is here considered to be the adsorbed CH_2 on an otherwise H-terminated surface (R in Figure 6), and the product is an adsorbed CH_3 with a neighboring radical carbon (P in Figure 6). An H is considered to be transferred from a surface carbon toward the adsorbed CH_2 species via a transition state structure (TS in Figure 6). An adsorbed CH_2 species on the surface can, hence, undergo two different surface reactions: the reaction with a migrating H or the insertion into a C−C dimer. It is therefore of greatest importance to also study the effect of substitutional N on this H migration reaction mechanism.

Effect by Substitutional N on Reaction Energy. As can be seen in Table 2, there are major differences for the reaction energies in the presence of substitutional N in specific positions. The reaction energies vary from −69 to 161 kJ/mol, which is to be compared with 10 kJ/mol for the undoped situation. Two major energetic effects are observed with N in the second carbon layer, positions 1 and 2. The H migration reaction is then favored by 69 kJ/mol and disfavored by 161 kJ/mol, respectively. For other positions of N, the reaction thermodynamic is only slightly affected by the presence of N. The reaction is energetically favored by 15 kJ/mol with N in the third and fourth carbon layers, position 1, while it is somewhat disfavored (about 18 kJ/mol) with N in the second carbon layer, position 3, and in the third carbon layer, position 2.

The more pronounced exothermic H migration with N in the second carbon layer, position 1, indicates that the situation with a CH_3 adsorbate and a neighboring surface radical C site is energetically more stable than a situation with CH_2 adsorbed on an otherwise fully H-terminated surface. This observation can be explained by the fact that the substitutional N atom is directly bonded to the surface C radical, thereby stabilizing this

specific structure. This result strengthens our conclusions made in the second part of Section III.2 that states that the surface structure will, compared to the situation with N further away, be more stable with N directly bonded to the surface radical C. The smaller effects for the other N positions can also be explained by the relative position of N. The fact that the H transfer reaction is strongly disfavored by N in carbon layer 2, position 2, can be explained by the β-scission rearrangement (discussed in Section III.2) that strongly stabilizes the surface structure with an adsorbed CH_2.

Effect by Substitutional N on Activation Energy. The presence of subsitutional N has here been shown to have a big effect on the activation energies calculated using Gaussian 03 (see Table 2). For most of the situations here described, a decrease in activation barrier for the H transfer reaction has been observed. This effect is obvious for N positioned within the second carbon layer, position 1, for which the activation energy is calculated to be around 5 kJ/mol (which is a lowering in energy of about 85 kJ/mol). This very small barrier means in practice that the adsorbed CH_2 species will rapidly react with the neighboring H species, thereby converting the adsorbate into CH_3. It will then hinder the C−C dimer insertion reaction for which an adsorbed CH_2 is a prerequisite. An energetic decrease in activation barrier was also found for N in the third and fourth carbon layers, position 1. The calculated activation barriers for these situations are about 34 kJ/mol (a lowering of about 56 kJ/mol). This somewhat smaller energetic decrease will also most probably speed up the formation of adsorbed CH_3 species and hence negatively affect the growth process. For N in layer 2, position 3, and in layer 3, position 2, the activation barrier for the H transfer reaction was found to be only slightly lowered compared to the undoped situation (78 and 69 kJ/mol vs 90 kJ/mol). However, the inverse reaction (i.e., the H migration from the CH_3 toward the neighboring surface carbon) is interesting to consider since it is thermodynamically more favored. For this inverse reaction, the activation barrier is found to be much lower compared to the undoped surface (23 (26) kJ/mol for NL2P3 (NL3P2) vs 87 kJ/mol). This decrease in activation energy implies that N in these specific positions will hinder the formation of adsorbed CH_3 by H migration toward an adsorbed CH_2. The large activation barrier (187 kJ/mol) observed for N in layer 2, position 2, is explained by the β-scission mechanism which strongly stabilizes the adsorbed CH_2 and thereby increases the activation energy.

Substitutional N shows a very strong effect on H migration between an adsorbed CH_2 species to a nearby positioned surface radical C. These lowering in activation energies can be explained by an interaction between the adsorbed CH_2 and the neighboring H adsorbate. The CH_2 species has an electron lone pair as a result of the electron transfer from the substitutional N toward CH_2. This CH_2−H interaction is visualized by the graphical representations of electron density differences in Figure 7. These representations clearly show that, for N in the second carbon layer, position 1, the positively charged surface H atom has been attracted by the lone pair somewhat localized between the CH_2 carbon and the H. With N in position 3, the electrons are observed to be more localized on the bond which connects CH_2 to the surface C. The interaction of CH_2 with the neighboring H is thereby weaker.

As a conclusion, a substitutional N generally decreases the activation barrier for the H transfer between an adsorbed CH_2 species and a nearby positioned surface radical C. The kinetics of this reaction is thereby expected to be energetically favored. However, the direction of this H transfer strongly depends on the N position, and the overall effect on the atomistic growth process needs further investigation.

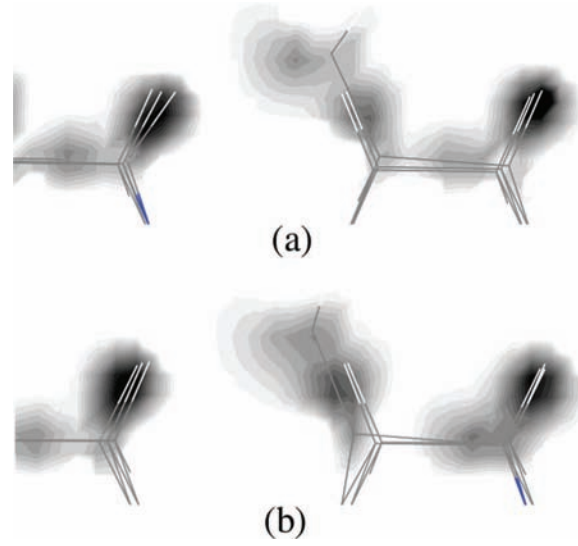

Figure 7. Electron density difference for CH_2 adsorbed on the surface with N in the second carbon layer position 1 (a) and 3 (b).

4. CH_2 Migration. ***CH_2 Migration for Nondoped Diamond.*** The migration reaction of CH_2 across dimer rows is based on the mechanism proposed by Frenklach et al.[25] and is considered to occur in two steps (see Figure 8). The first migration step (R → I) corresponds to the inverse of the CH_2 insertion reaction, discussed in Section III.2. The main difference is that, as a result of the reaction, the adsorbed radical CH_2 is positioned very close to the neighboring surface carbon radical. The proximity of these two C radicals induces a rapid formation of a new C−C bond that forms the finally bridged structure. This rapid formation constitutes the second step (I → P) in the migration process.

The calculated reaction and activation energies are presented in Table 3. For the first reaction step, the reaction energies are consistent with the values calculated for the C−C dimer insertion reaction considering that migration is the forward and insertion is the inverse direction of the same reaction (ΔE = 28 kJ/mol and ΔE^* = 140 kJ/mol vs ΔE = −20 kJ/mol and ΔE^* = 107 kJ/mol, where ΔE and ΔE * are the reaction energies and activation barriers, respectively). The similarities between the reaction energies and the activation barriers indicate that the presence of a neighboring surface C radical is not affecting this specific reaction step (i.e., step 1). The following step (i.e., step 2) is energetically favored (by about −107 kJ/mol) due to the formation of a new bond within the bridged structure. An analysis of the surface structure indicates that the neighboring C−C bonds within the two connected dimers will be stretched (by about 1.94 Å). This value is to be compared with the value for a C−C dimer on a ordinary (100)-2 × 1 H-terminated surface: 1.62 Å. Despite this rather long C−C distance, a stabilizing interaction is expected to be present between these two C atoms since an overall strong energetic stabilization of the whole system has been observed. The very low activation barrier that has been calculated for TS2 (of about 12 kJ/mol) indicates that the second migration step reaction will occur with a high probability.

Effect by Substitutional N on the CH_2 Migration. *Reaction Step 1.* As can be seen in Table 3, the reaction energy calculated for the first step is observed to be very similar to the energy calculated for the undoped situation (between 18 and 38 kJ/mol vs 28 kJ/mol). However, two exceptions can be observed

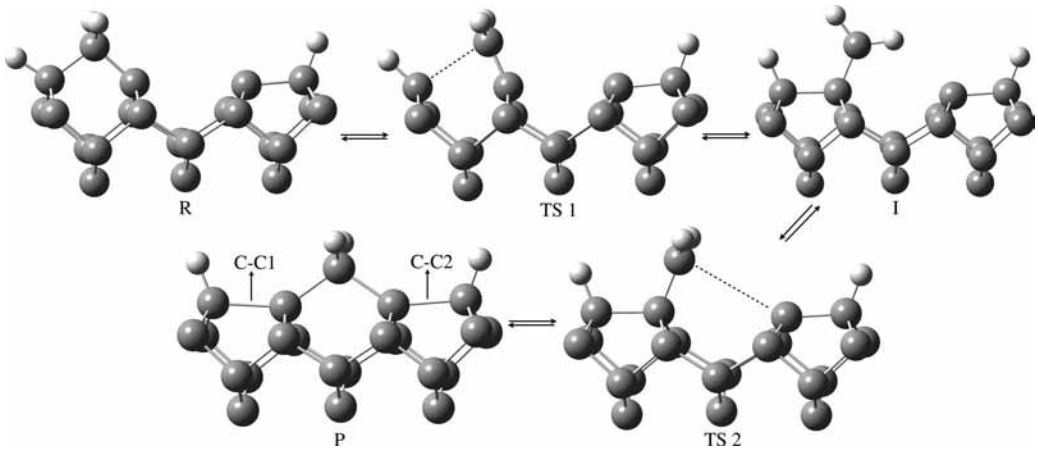

Figure 8. CH_2 migration reaction from an inserted position within a carbon dimer toward a bridged position between two C−C dimers. R, I, and P represent the reactant, intermediate, and product structures, respectively. TS1 and TS 2 represent the two transition states.

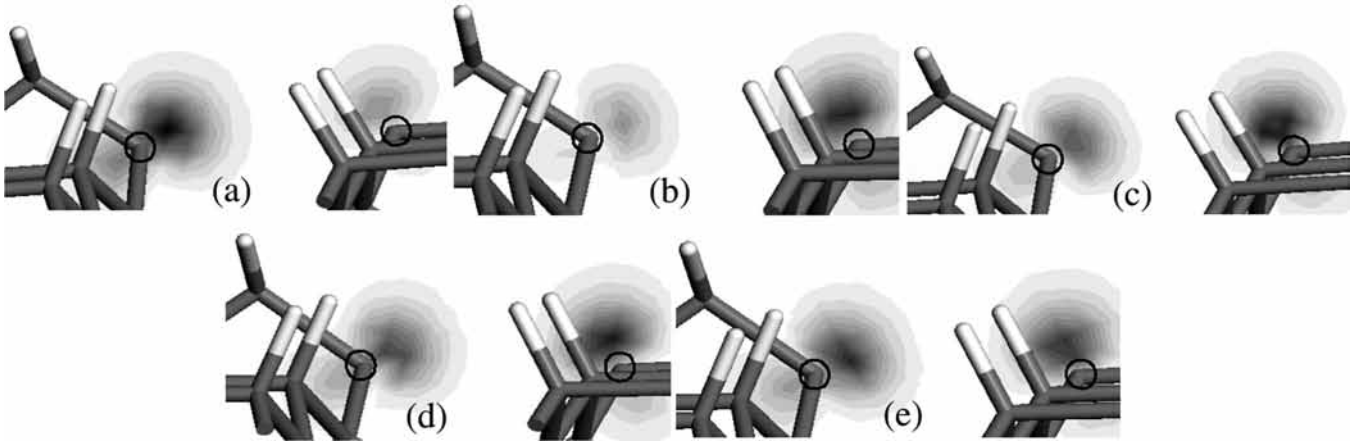

Figure 9. Representation of the spin densities on the two surface carbon radicals (highlighted with black circles) within the initial reactant structure (R in Figure 8). N is positioned within the second carbon layer, position 1 (a), 2 (b), and 3 (c), and with within the third (d) and fourth (e) carbon layers, position 1.

TABLE 3: Reaction Energies (ΔE) and Activation Barriers (ΔE^*) for the First (R1) and Second (R2) Reaction Steps within the CH_2 Surface Migration Process

CH_2 migration (kJ/mol)		no N	NL2P1	NL2P2	NL2P3	NL3P1	NL3P2	NL4P1	NL4P2
DMol[3]	ΔE_{R1}	28.1	20.1	−64.0	8.5	38.2	67.8	22.2	17.8
	ΔE_{R2}	−106.5	30.7	92.8	−15.6	−8.7	−35.4	18.2	1.9
Gaussian	ΔE_{R1}	21.0	34.0	−49.4	32.0	51.9	117.2	35.9	–
	ΔE_{R2}	−92.7	49.3	108.8	−41.8	−5.3	−56.8	33.3	–
	ΔE^*_{R1}	139.9	154.2	251.1	125.0	188.6	273.9	182.6	–
	ΔE^*_{R2}	12.4	92.6	154.2	11.0	43.9	150.9	78.6	–

with N in position 2 in the second and third carbon layers (with reaction energies of about −64 and 67 kJ/mol). These energetic differences can be easily explained by β-scission reconstructions which stabilize the surface when N is in β-position with respect to the surface radical. For N in the second carbon layer, position 2, the reconstruction takes place after the first reaction step, which results in an adsorbed position of CH_2 and an overall exothermic reaction. The situation is opposite for N in the third carbon layer, position 2. For this situation, the β-scission reconstruction occurs with CH_2 inserted into the C−C dimer, resulting in an overall endothermic reaction.

As can be seen in Table 3, the activation energies are observed to be only slightly affected by the presence of N in the second carbon layer, positions 1 and 3 (about 154 and 125 kJ/mol for NL2P1 and NL2P3). This is to be compared with a value of 140 kJ/mol for the undoped situation. For the other N positions, the activation barriers are increased by the presence of the dopant: 251, 189, 274, and 183 kJ/mol for NL2P2, NL3P1, NL3P2, and NL4P1, respectively. With N in the second carbon layer, position 1, N is directly bonded to the carbon radical within the dimer neighboring the reaction site. The analysis of the spin density shows that the extra electron from N is predominantly located on the surface radical carbon directly connected to N (demonstrated as a very low spin density on the surface carbon to the right in Figure 9a). The reaction is thereby not affected by the presence of the dopant, and the activation barrier is similar in energy to the undoped situation. This can be confirmed by a structural analysis of the transition structure. The C−C distance, represented with a dashed line in TS1 in Figure 8, is increasing with an increased electrostatic repulsion between the two carbon atoms. This will affect the stability of the transition state structure, as discussed in Section

III.2. The distance between these two carbons is calculated to be 2.38 Å, which is similar to 2.31 Å for the undoped situation.

The spin density analysis with N in the second carbon layer, position 3, indicates that the extra electron in N is predominantly localized on the surface carbon radical that is participating in the reaction (the spin density is lower on the carbon to the left in Figure 9c). The substitutional N will thereby affect the CH_2 migration reaction. As observed for the C−C dimer insertion reaction, N in that specific position tends to slightly reduce the activation barrier.

With N in the second carbon layer, position 2, the extra N electron is directly transferred to the surface radical C involved in the first step of the migration reaction. The spin density plot shows clearly that the spin density is lower on that specific carbon (radical carbon to the left in Figure 9b). As a result for the TS structure, the C−C distance (represented with a dashed line in Figure 8) will be increased due to electrostatic repulsions (2.63 Å for NL2P2 vs 2.31 Å for the undoped surface). The transition state structure will thereby be destabilized, which furthermore will explain the higher activation barrier.

With N in the third and fourth carbon layers, position 1, the spin density presents an intensity which is similar for both surface carbons (Figures 9d and e). It indicates that the extra electron from N will not be localized, but shared by both surface radical carbons. The reaction barrier becomes higher due to an increase in electrostatic repulsion between the two C's involved in the bond breakage. As mentioned in Section III.2, this repulsion is responsible for the destabilization of the transition state structure. A structural analysis further supports these observations by a larger distance obtained between the two carbons connected with a dashed line in Figure 8 (2.52 Å for NL3P1 and 2.48 Å for NL4P1 vs 2.31 Å for the undoped surface).

The large activation barrier calculated for N in the third carbon layer, position 2 (of about 274 kJ/mol), is easily explained by the β-scission rearrangement which takes place when CH_2 is inserted into the C dimer prior to the migration reaction. This rearrangement strongly stabilizes the reactant structure and thereby induces an increase in the energy barrier.

Reaction Step 2. The reaction energies for the second reaction step (i.e., the formation of a bridged structure) are presented in Table 3. Rather large energetic variations can be observed by the presence of N within the surface. The reaction, which induces an energetic exothermic energy value of 108 kJ/mol for an undoped situation, becomes less energetically favored with N in the second carbon layer, position 3 (by about 16 kJ/mol), and with N in the third carbon layer, positions 1 and 2 (by about 9 vs 35 kJ/mol). On the other hand, N in the second and the fourth carbon layers, position 1 and 2, is observed to disfavor the second step of the migration reaction (an increase of about 31, 93, 18, and 2 kJ/mol for NL2P1, NL2P2, NL4P1, and NL4P2, respectively).

With N in the second, or third, carbon layer in position 2, the larger differences in reaction energy can again be explained by the β-scission mechanism, which takes place before the reaction for the NL2P2 situation, and both before and after the reaction for NL3P2. With N in the third carbon layer, position 1, N is also in β-position with respect to the surface radical carbon after the reaction. A β-scission reconstruction is then observed to take place which induces the stabilization of the surface and, hence, an observed weak exothermicity of the reaction.

An analysis of the final bridged surface structure shows, compared to the undoped situation, apparent changes in the presence of N. From Table 4 it can be observed that the C−C distances are equal for both neighboring dimers on the undoped surface. This symmetry in dimer bond length is kept for the situation with N within the third and fourth carbon layers, position 1. However, the distances are significantly increased. This elongation can be explained by the occupation of the antibonding orbitals of the C−C bonds of the dimers. With N in the second (position 1 and 4) and fourth carbon layers (position 2), only one C−C dimer bond is elongated. This also has to do with the occupation of the antibonding orbital. While nitrogen is positioned so that it has identical distances to the two dimers for the NL3P1 and NL4P1 scenarios, N is positioned closer to one of the C−C dimers for NL2P1, NL2P3, and NL4P2, respectively. It can be observed that the longest C−C bond is the one which is closest to the substitutional N for these latter cases. The extra N electron is being predominantly localized within the closest C−C dimer bond, which thereby becomes elongated. It is worth noticing that the C−C bond within the other dimer to which CH_2 is bonded in a bridge formation will become shorter compared to the undoped situation.

TABLE 4: Length of the Carbon Dimer Bonds C−C1 and C−C2 for the Bridged Structure in Figure 8 (Structure P)

bond length (Å)	no N	NL2P1	NL2P3	NL3P1	NL4P1	NL4P2
C−C1	1.94	1.82	2.49	2.29	2.26	2.51
C−C2	1.94	2.49	1.80	2.30	2.27	1.84

For N in the second, third, and fourth carbon layers, position 1, the increase in activation barrier can be explained by the presence of the extra N electron on the reactive surface carbon, onto which CH_2 will bind. A resulting electrostatic repulsion has been observed between the negatively charged C (in CH_2) and the surface carbon containing the electron lone pair.

With N in the second carbon layer, position 3, a structural analysis of the surface indicates that the intermediate structure prior to the second reaction step is "activated" due to the presence of a substitutional N. The C−C dimer bond is longer compared to the other N positions (1.96 Å vs 1.72 Å within NL2P1), and the C−CH_2 bond becomes shorter (1.43 Å vs 1.48 Å within NL2P1). This surface destabilization that takes place before the reaction thereby explains the exothermicity of the reaction and the low activation barrier.

In conclusion, the study of the CH_2 migration reaction shows that the effect of a substitutional N within the second carbon layer is very local. The extra electron from the substitutional N will only be transferred toward the closest surface carbon radical, and a second radical present on the surface will not be affected. If that surface carbon radical, to where the electron is transferred, is not involved in the reaction, the effect of N on this reaction will be negligible. With N in the third and fourth carbon layers, the extra electron from substitutional N is observed to be delocalized on both surface radicals which generally disfavors the CH_2 migration reaction. Substitutional N is thereby observed to negatively influence the surface migration of CH_2 species.

IV. Conclusions

Within the present work, the effect of substitutional N on three important diamond growth reaction steps has been carefully investigated using quantum mechanical methods. The calculations are based on density functional theory (DFT), using both cluster and periodic models. The following reactions have been considered for the diamond (100) growth: (i) CH_2 insertion within a carbon dimer, (ii) H transfer from a neighboring surface carbon to an adsorbed CH_2, and (iii) surface migration of CH_2.

For the CH_2 insertion reaction, the reaction energies in the presence of N were calculated to be generally similar to the energy obtained for an undoped surface. Some exceptions were, however, observed when N is in β-position with respect to a surface carbon radical. The surface was thereby stabilized by a β-scission reconstruction which largely affects the reaction energy. The reaction is observed to be favored or disfavored depending on this lateral position. On the other hand, the reaction activation energies were with one exception observed to be significantly increased by the presence of substitutional N. The situation with N in the second carbon layer, position 3, resulted in a slightly lower energy barrier. In summary, our results showed that N has a negative effect on the kinetics of this specific insertion reaction, being a crucial growth step within the generally accepted mechanism initially proposed by Goodwin et al.

The presence of N was observed to strongly affect both the reaction energy and the activation barrier for the H migration reaction. It was especially found that the effect of N on H migration is only sensitive to the lateral position of N, and not at all to the choice of carbon layer. For an adsorbed CH_2 on the surface, its transformation to an adsorbed CH_3 will hence be strongly dependent on only the lateral position of the substitutional N. When the CH_3 formation is energetically favored, the growth process is expected be negatively affected. The corresponding activation barriers were observed to be smaller in the presence of N, which is a circumstance that is expected to strongly favor the reaction kinetics.

For the CH_2 migration reaction, the substitutional N was observed to increase the activation barriers for the two partial reaction steps, thereby negatively affecting the reaction kinetics. It is worth mentioning that, with N in the second carbon layer, the extra N electron will be localized on only one of the two surface carbon radicals present on the surface. However, with N in the third or the fourth carbon layer, the extra electron is observed to be delocalized over the two surface radicals.

The limited size of the model used within this study corresponds to a high substitutional N concentration. However, the aim with the present study was not to focus on the effect of N concentration but on the effect of nearby positioned N on the most important growth steps within the diamond synthesis. In the presence of N, the general increase in activation barriers and occurrence of β-scission rearrangements, inducing the formation of C−C double bonds, could be an explanation for the surface degradation and the decrease in growth rate observed experimentally with large nitrogen concentration in the gas phase.

Acknowledgment. This work was supported by the European Project RTN DRIVE from the 6th Framework Program (no. MRTN-CT-2004-512224). The results were generated using DMol^3 within the program package Material Studio, developed by Accelrys Inc., San Diego, CA.

References and Notes

(1) Angus, J. C.; Hayman, C. C. *Science* **1988**, *241*, 913–921.
(2) Williams, O.; Nesladek, M. *Phys. Status Solidi* **2006**, *203*, 3375–3386.
(3) Werner, M.; Locher, R. *Rep. Prog. Phys.* **1998**, *61*, 1665–1710.
(4) Silva, F.; Bonnin, X.; Achard, J.; Brinza, O.; Michau, A.; Gicquel, A. *J. Cryst. Growth* **2008**, *310*, 187–203.
(5) Goodwin, D. G.; Butler, J. E. Theory of diamond chemical vapor deposition. In *Handbook of industrial diamonds and diamond films*; Prelas, G. P. M. A., Bigelow, L. K., Eds.; Marcel Dekker, Inc: New York, 1997; pp 527−581.
(6) Wild, C.; Kohl, R.; Herres, N.; Müller-Sebert, W.; Koidl, P. *Diamond Rel. Mater.* **1994**, *3*, 373–381.
(7) Locher, R.; Wild, C.; Herres, N.; Behr, D.; Koidl, P. *Appl. Phys. Lett.* **1994**, *65*, 34–36.
(8) Jin, S.; Moustakas, T. D. *Appl. Phys. Lett.* **1994**, *65*, 403–405.
(9) Cao, G.; Schermer, J.; van Enckevort, W.; Elst, W.; Giling, L. *J. Appl. Phys.* **1996**, *79*, 1357–1364.
(10) Silva, F.; Gicquel, A. *Electrochem. Soc.* **1998**, *97*, 99–125.
(11) Benedic, F.; Belmahi, M.; Elmazria, O.; Assouar, M. B.; Fundenberger, J.-J.; Alnot, P. *Surf. Coat. Technol.* **2003**, *176*, 37–49.
(12) Butler, J. E.; Oleynik, I. *Philos. Trans. R. Soc.London* **2008**, *366*, 295–311.
(13) Battaile, C. C.; Srolovitz, D. J.; Butler, J. E. *Diamond Rel. Mater.* **1997**, *6*, 1198–1206.
(14) Battaile, C. C.; Srolovitz, D. J.; Butler, J. E. *J. Appl. Phys.* **1997**, *82*, 6293–6300.
(15) Bachelet, G. B.; Baraff, G. A.; Schlüter, M. *Phys. Rev. B* **1981**, *24*, 4736–4744.
(16) Briddon, P. R.; Jones, R. *Physica B* **1993**, *185*, 179–189.
(17) Larsson, K. *Comp. Mater. Sci.* **2003**, *27*, 23–29.
(18) Frauenheim, Th.; Jungnickel, G.; Sitch, P.; Kaukonen, M.; Weich, F.; Widany, J.; Porezag, D. *Diamond Rel. Mater* **1998**, *7*, 348–355.
(19) Sitch, P. K.; Jungnickel, G.; Kaukonen, M.; Porezag, D.; Frauenheim, Th.; Pederson, M. R.; Jackson, K. A. *J. Appl. Phys.* **1998**, *83*, 4642–4646.
(20) Van Regemorter, T.; Larsson, K. *Chem. Vap. Deposit.* **2008**, *14*, 224–231.
(21) Garrison, B. J.; Dawnkaski, E. J.; Srivastava, D.; Brenner, D. W. *Science* **1992**, *255*, 835–838.
(22) Harris, S. J.; Goodwin, D. G. *J. Phys. Chem.* **1993**, *97*, 23–28.
(23) Tamura, H.; Gordon, M. S. *Chem. Phys. Lett.* **2005**, *406*, 197–201.
(24) Skokov, S.; Weiner, B.; Frenklach, M. *J. Phys. Chem.* **1994**, *98*, 7073–7082.
(25) Frenklach, M.; Skokov, S. *J. Phys. Chem. B* **1997**, *101*, 3025–3036.
(26) Netto, A.; Frenklach, M. *Diamond Relat. Mater.* **2005**, *14*, 1630–1646.
(27) (a) Delley, B. *J. Chem. Phys.* **1990**, *92*, 508–517. (b) Delley, B. *J. Chem. Phys.* **2000**, *113*, 7756–7764.
(28) Frisch, M. J.; Trucks, G. W.; Schlegel, H. B.; Scuseria, G. E.; Robb, M. A.; Cheeseman, J. R.; Montgomery J. A., Jr.; Vreven, T.; Kudin, K. N.; Burant, J. C.; Millam, J. M.; Iyengar, S. S.; Tomasi, J.; Barone, V.; Mennucci, B.; Cossi, M.; Scalmani, G.; Rega, N.; Petersson, G. A.; Nakatsuji, H.; Hada, M.; Ehara, M.; Toyota, K.; Fukuda, R.; Hasegawa, J.; Ishida, M.; Nakajima, T.; Honda, Y.; Kitao, O.; Nakai, H.; Klene, M.; Li, X.; Knox, J. E.; Hratchian, H. P.; Cross, J. B.; Bakken, V.; Adamo, C.; Jaramillo, J.; Gomperts, R.; Stratmann, R. E.; Yazyev, O.; Austin, A. J.; Cammi, R.; Pomelli, C.; Ochterski, J. W.; Ayala, P. Y.; Morokuma, K.; Voth, G. A.; Salvador, P.; Dannenberg, J. J.; Zakrzewski, V. G.; Dapprich, S.; Daniels, A. D.; Strain, M. C.; Farkas, O.; Malick, D. K.; Rabuck, A. D.; Raghavachari, K.; Foresman, J. B.; Ortiz, J. V.; Cui, Q.; Baboul, A. G.; Clifford, S.; Cioslowski, J.; Stefanov, B. B.; Liu, G.; Liashenko, A.; Piskorz, P.; Komaromi, I.; Martin, R. L.; Fox, D. J.; Keith, T.; Al Laham, M. A.; Peng, C. Y.; Nanayakkara, A.; Challacombe, M.; Gill, P. M. W.; Johnson, B.; Chen, W.; Wong, M. W.; Gonzalez, C.; Pople, J. A. *Gaussian 03*, Revision E.01; Gaussian, Inc.: Wallingford, CT, 2004.
(29) Van Regemorter, T.; Larsson, K. *J. Phys. Chem. A* **2008**, *112*, 5429–5435.
(30) Becke, A. D. *Phys. Rev. A* **1988**, *38*, 3098–3100.
(31) Lee, C.; Yang, W.; Parr, P. R. **1988**, *37*, 785–789.
(32) Pfrommer, B. G.; Côté, M.; Louie, S. G.; Cohen, M. L. *J. Comput. Phys.* **1997**, *131*, 233–240.
(33) Monkhorst, H. J.; Pack, J. D. *Phys. Rev. B* **1976**, *13*, 5188–5192.
(34) D Becke, A. *J. Chem. Phys.* **1993**, *98*, 5648–5652.
(35) (a) Peng, C. Y.; Ayala, P. Y.; Schlegel, H. B.; Frisch, M. J. *J. Comput. Chem.* **1996**, *17*, 49–56. (b) Peng, C. Y.; Schlegel, H. B. *Isr. J. Chem.* , *33*, 449–454.
(36) Reed, A. E.; Weinstock, R. B.; Weinhold, F. *J. Chem. Phys.* **1985**, *83*, 735–746.
(37) Cheesman, A.; Harvey, J. N.; Ashfold, M. N. R. *J. Phys. Chem. A* **2008**, *45*, 11436–11448.
(38) Kang, J. K.; Musgrave, C. B. *J. Chem. Phys.* **2000**, *113*, 7582–7587.
(39) Larsson, K.; Carlsson, J.-O. *Phys. Rev. B* **1999**, *59*, 8315–8322.
(40) Dawnkaski, E. J.; Srivastava, D.; Garrison, B. J. *Chem. Phys. Lett.* **1995**, *232*, 524–530.
(41) Skokov, S.; Weiner, B.; Frenklach, M. *J. Phys. Chem.* **1994**, *98*, 8–11.
(42) Gali, A.; Mészáros, A.; Deák, P. *Diamond Relat. Mater.* **1996**, *5*, 613–616.
(43) van Enckevort, W. J. P.; Janssen, G.; Vollenberg, W.; Schermer, J. J.; Giling, L. J.; Seal, M. *Diamond Relat. Mater.* **1993**, *2*, 997–1003.
(44) Lee, N.; Badzian, A. *Diamond Relat. Mater.* **1997**, *6*, 130–145.

(45) Achard, J.; Silva, F.; Tallaire, A.; Bonnin, X.; Lombardi, G.; Hassouni, K.; Gicquel, A. *J. Phys. D: Appl. Phys.* **2007**, *40*, 6175–6188.

(46) Battaile, C. C.; Srolovitz, D. J.; Oleinik, I. I.; Pettifor, D. G.; Sutton, A. P.; Harris, S. J.; Butler, J. E. *J. Chem. Phys.* **1999**, *111*, 4291–4299.

(47) Frenklach, M.; Skokov, S.; Weiner, B. *Nature* **1994**, *372*, 535–537.

(48) D'Evelyn, M. P.; Graham, J. D.; Martin, L. R. *J. Cryst. Growth* **2001**, *231*, 506–519.

(49) Aylward, G. Findlay, T. *SI Chemical Data*, 3rd ed.; John Wiley & Sons: New York, 1994.

JP811505W